

Chou-Yang Model and Hyperon-Proton Elastic Scattering

Mohammad Saleem,⁽¹⁾ Muhammad Rafique,⁽²⁾ Haris Rashid,⁽¹⁾ and Fazal-e-Aleem⁽¹⁾

⁽¹⁾Centre for High Energy Physics, Punjab University, Lahore-20, Pakistan

⁽²⁾Department of Mathematics, Punjab University, Lahore-20, Pakistan

(Received 15 August 1986)

By use of the electromagnetic form factors for Ξ^- , Σ^- , Σ^+ , and Ω^- computed recently from lattice quantum chromodynamics, the Chou-Yang model has been applied to explain and/or predict the differential cross section and other characteristics of Ξ^-p , $\Sigma^\pm p$, and Ω^-p elastic reactions.

PACS numbers: 13.85.Dz, 12.40.Pp

The preliminary version of the Chou-Yang model proposed for proton-proton elastic scattering at high energies¹ predicted a dip in the differential cross section at $-t \approx 1.4$ (GeV/c)² and a second dip near $-t = 6$ (GeV/c)². The first dip was observed two years later and gave a boost to the model; the second dip has not been observed although measurement of differential cross section in pp elastic scattering has been extended beyond $-t \approx 10$ (GeV/c)². The experimental rise of σ_{el}/σ_T in going from CERN Intersecting Storage Ring to CERN Collider energies² has been another favorable point for this model.

Recently, Lombard and Tellaz-Arnas³ have tried to explain the $p\alpha$ and $\alpha\alpha$ elastic scattering by using the pristine Chou-Yang model. Since the form factor for the α particle is also known, the scattering amplitude could be evaluated. In fact, they choose an exponential form of the proton form factor, which is very much consistent with the experimental measurements up to $-t \approx 1.6$ (GeV/c)². This facilitates the computation. These authors have observed a qualitative agreement with the experimental data. Lombard and Wilkin⁴ have also extracted the form factors of the proton and the π and K mesons from high-energy pp , $\pi^\pm p$, and $K^\pm p$ elastic-scattering data on the basis of the Chou-Yang model. However, the model has not yet been used to explain the various characteristics of hyperon-proton elastic scattering. This is because electromagnetic form factors of hyperons were not available. The experimental measurements of these form factors have not yet been made. But very recently Samuel and Moriarty⁵ have used lattice quantum chromodynamics to compute the electromagnetic form factors and we have made use of the corresponding expressions to apply the Chou-Yang model to (charged) hyperon-proton reactions. The electromagnetic form factor has a precise definition in terms of the matrix element of the electromagnetic current. In the low-momentum region, the form factor is also given by the Fourier transform of the charge density:

$$F(Q^2) = \int d^3r \exp(i\mathbf{Q} \cdot \mathbf{r}) \rho(\mathbf{r}).$$

This equation was used to compute electromagnetic form factors of baryons in the low-energy regime ($0 < Q < 2$ GeV/c). Only electromagnetic form factors of nucleons

have been measured experimentally. In the case of the proton, their calculations⁵ fit the experimental results⁶ well, although they are slightly above the data in the $Q \approx 0.6$ GeV/c range. For the neutron, however, Ref. 5 gives zero for the form factor which is in strong disagreement with the experimental data. Nevertheless, the predictions in lattice QCD for charged hyperons may be used as good representations of the form factors until experimental determinations become available.

The lattice-QCD-based computed values of the electromagnetic form factors can be well represented by the following expressions: For Ξ^- ,

$$F(t) = -e^{1.12t + 0.035t^2},$$

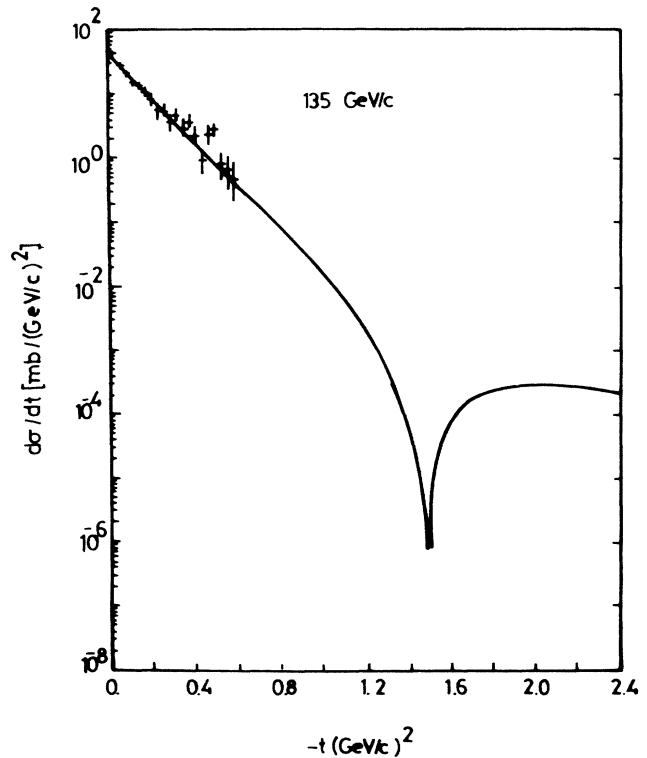


FIG. 1. Differential cross sections for $\Xi^-p \rightarrow \Xi^-p$ plotted vs $-t$. The experimental points have been taken from Ref. 7. The solid line represents the results of the Chou-Yang model.

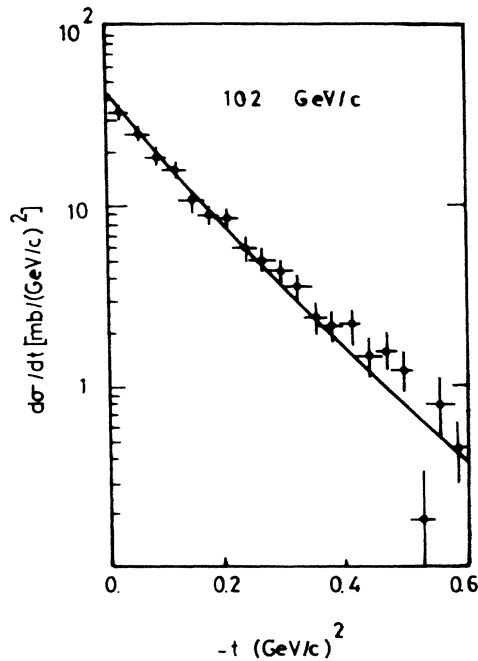


FIG. 2. Differential cross section for $\Xi^-p \rightarrow \Xi^-p$ plotted vs $-t$. The experimental points have been taken from Ref. 7. The solid line represents the results of the Chou-Yang model.

for Σ^- ,

$$F(t) = -e^{0.98t + 0.04t^2};$$

for Σ^+ ,

$$F(t) = 0.8e^{1.55t} + 0.23e^{-t^2} - 0.03;$$

for Ω^- ,

$$F(t) = -e^{0.93t + 0.045t^2};$$

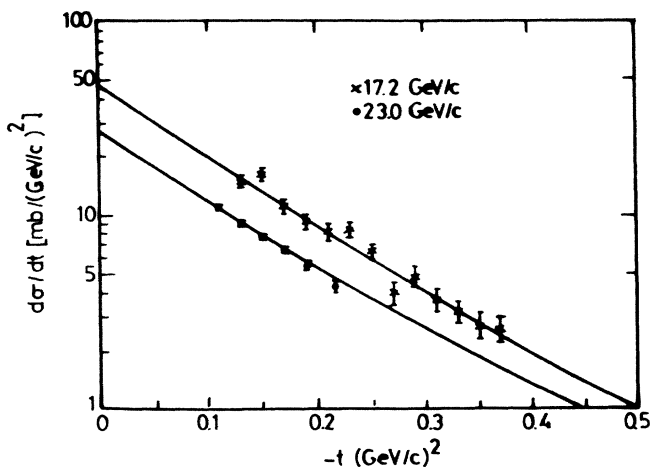


FIG. 3. Differential cross section for $\Sigma^-p \rightarrow \Sigma^-p$ plotted vs $-t$, at 17.0 and 23 GeV/c. The experimental points have been taken from Refs. 8 and 9. The solid curves represent the predictions of the model described in the text.

where $-t = Q^2$, and t is in (GeV/c).

Since the total cross sections at high energies for Ξ^-p and Σ^-p scattering have been measured experimentally,⁷ we are now in a position to calculate $d\sigma/dt$ and other characteristics of these reactions by using the Chou-Yang model. For other reactions, for given σ_T , predictions can be made for differential cross sections, etc. We have used the dipole form factor for the proton throughout this work.

For Ξ^-p , by adjusting K so as to yield the total cross section consistent with the measured value of 29.35 ± 0.31 mb, we obtain the differential-cross-section curve which, along with the experimental data⁸ at 135 GeV/c, is shown in Fig. 1. There is a very good agree-

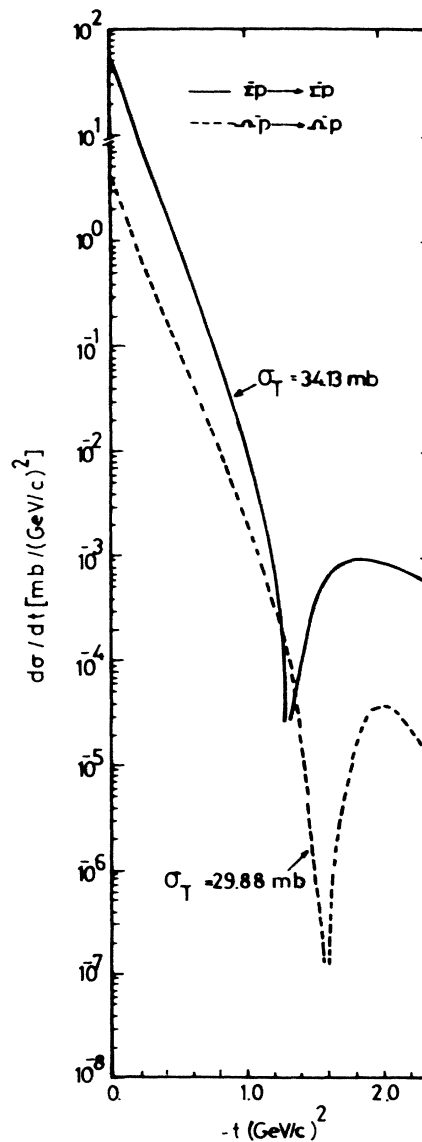


FIG. 4. Differential-cross-section predictions of the model for the reactions $\Sigma^-p \rightarrow \Sigma^-p$ and $\Omega^-p \rightarrow \Omega^-p$ at $\sigma_T = 34.13$ and 29.88 mb, respectively.

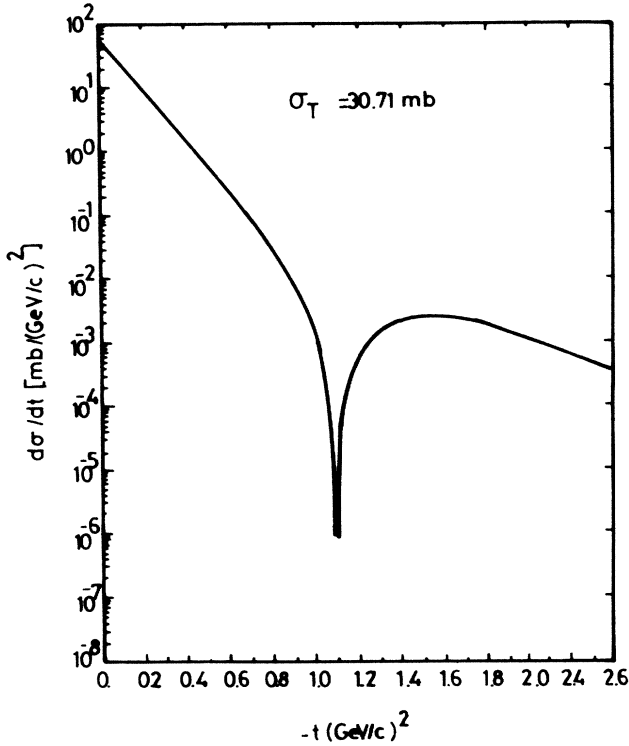


FIG. 5. Differential-cross-section predictions of the model for the reaction $\Sigma^+p \rightarrow \Sigma^+p$ at $\sigma_T = 30.71$ mb.

ment with experiment endorsing the validity of the electromagnetic form factor for Ξ^- lattice QCD. We also notice that the differential cross section shows a zero near $-t = 1.5$ $(\text{GeV}/c)^2$, rises up to $-t \approx 2.0$ $(\text{GeV}/c)^2$, and then starts falling again. The values up to $-t = 2.4$ $(\text{GeV}/c)^2$ are shown in the figure. In fact, we have not considered the real part of the scattering amplitude. This could be done only if either ρ (the ratio of the real and imaginary parts of the scattering ampli-

tude at $t=0$) or $d\sigma/dt$ in the vicinity of zero were experimentally known. We expect that this real part of the scattering amplitude would partially fill this zero so as to form a dip.

Figure 2 shows the fit of the experimental data⁸ for $\Xi^-p \rightarrow \Xi^-p$ with the prediction of the Chou-Yang model at 102 GeV/c, corresponding to $\sigma_T = 29.19 \pm 0.29$ mb.

The differential cross section for $\Sigma^-p \rightarrow \Sigma^-p$ has been measured at 17.0 and 23.0 GeV/c.^{9,10} We have adjusted the value of K so as to give the values of σ_T as 30.37 and 22.29 mb, respectively. The differential-cross-section results obtained by use of the Chou-Yang model agree very well with the experimental data. This is shown in Fig. 3. The σ_T results show that these measurements have been made in the range where the total cross section is falling with energy. The total cross sections for this reaction are available at various high momenta ranging from 74.5 to 136.9 GeV/c.⁷ Therefore the Chou-Yang model can be used to predict differential cross section and other characteristics of this reaction. We have calculated the differential cross section for $\sigma_T = 34.13$ mb, corresponding to 136.9 GeV/c, and drawn the theoretical curve in Fig. 4. The curve exhibits a behavior similar to that of Ξ^-p elastic scattering. The dip in this case occurs near $-t = 1.3$ $(\text{GeV}/c)^2$, while a bump occurs at $-t \approx 1.9$ $(\text{GeV}/c)^2$. The $d\sigma/dt$ measurements corresponding to this value of σ_T would further endorse the validity of the Σ^- form factor computed in Ref. 5.

Figure 4 also shows the predicted values of the differential cross section for Ω^-p elastic scattering corresponding to $\sigma_T = 29.88$ mb. The experimental data are not available for this reaction but we expect a dip (when the real part is included) in the vicinity of $-t = 1.6$ $(\text{GeV}/c)^2$.

The experimental data for Σ^+p elastic scattering are

TABLE I. Theoretical values of σ_{el} and B for charged hyperon-proton elastic reactions for various momenta or total cross sections. Experimental values wherever available are shown for comparison.

Reaction	Momentum or total cross section	σ_{el} (mb)		B $(\text{GeV}/c)^2$	
		Expt.	Theor.	Expt.	Theor.
$\Xi^-p \rightarrow \Xi^-p$	102 GeV/c	4.9 ± 0.7^a	5.12	7.7 ± 0.4^a (0.01-0.42)	8.20, $0.01 \leq -t \leq 0.42$
	135 GeV/c	5.6 ± 0.9^a	5.17	8.2 ± 0.5^a (0.01-0.42)	8.21, $0.01 \leq -t \leq 0.42$
$\Sigma^-p \rightarrow \Sigma^-p$	17 GeV/c	...	5.64	8.12 ± 0.35^b (0.12-0.38)	7.83, $0.12 \leq -t \leq 0.38$
	23 GeV/c	...	3.25	8.99 ± 0.31^c (0.1-0.23)	7.54, $0.1 \leq -t \leq 0.23$
$\Omega^-p \rightarrow \Omega^-p$	$\sigma_T = 34.13$ mb	...	6.94	...	8.9, $0 \leq -t \leq 0.1$
	$\sigma_T = 29.88$ mb	...	5.57	...	4.25, $0 \leq -t \leq 0.1$
$\Sigma^+p \rightarrow \Sigma^+p$	$\sigma_T = 30.71$ mb	...	5.43	...	9.0, $0 \leq -t \leq 0.05$

^aReference 7.
^bReference 8.

^cReference 9.

also not available. We can, however, predict differential cross sections for this reaction at any given total cross section. Figure 5 shows specimen results corresponding to $\sigma_T = 30.71$ mb. The zero in the differential-cross-section curve occurs at $-t \approx 1.1$ (GeV/c)².

The predicted values of σ_{el} and B at momenta corresponding to various total cross sections and for different reactions along with the experimental data wherever available are shown in Table I. The agreement is quite satisfactory.

The above analysis shows that the agreement between the predicted values and the available experimental data for various characteristics of hyperon-proton elastic reactions is satisfactory. Since only the low-momentum part is tested, it is a success for the lattice-QCD calculations. It would be very interesting to see what will happen at higher momentum transfer.

Financial assistance from the Pakistan Science Foundation under Contract No. P-PU/Phys(11/2) is gratefully acknowledged.

¹T. T. Chou and C. N. Yang, Phys. Rev. **170**, 1591 (1968), and Phys. Rev. Lett. **20**, 1213 (1968); L. Durand and R. Lipes, Phys. Rev. Lett. **20**, 637 (1968).

²M. Bozzo *et al.*, Phys. Lett. **147B**, 392 (1984); A. Breakstone *et al.*, Nucl. Phys. **B248**, 253 (1984).

³R. J. Lombard and A. Tellaz-Arenas, Phys. Lett. **165B**, 205 (1985).

⁴R. J. Lombard and C. Wilkin, J. Phys. G **3**, L5 (1977).

⁵S. Samuel and K. J. M. Moriarty, CERN, Report No. CERN-TH-4396/86, 1986 (to be published).

⁶M. Gourdin, Phys. Rep. **11**, 29 (1979); E. E. Chambers and R. Hofstadter, Phys. Rev. **103**, 1454 (1956); K. W. Chen *et al.*, Phys. Rev. **141**, 1267 (1966); T. Janssens *et al.*, Phys. Rev. **142**, 922 (1966); L. E. Price *et al.*, Phys. Rev. D **4**, 45 (1971); P. N. Kirk *et al.*, Phys. Rev. D **8**, 63 (1973); W. Bartel *et al.*, Nucl. Phys. **B58**, 429 (1973).

⁷S. F. Biagi *et al.*, Nucl. Phys. **B186**, 1 (1981).

⁸S. F. Biagi *et al.*, Z. Phys. C **17**, 113 (1983).

⁹J. J. Blaising *et al.*, Phys. Lett. **58B**, 121 (1975).

¹⁰R. D. Majka *et al.*, Phys. Rev. Lett. **37**, 413 (1976).